SYNTHESIS OF SAN FERNANDO STRONG-MOTION RECORDS

Thomas H. Heaton and Donald V. Helmberger

Seismological Laboratory
California Institute of Technology

Three-dimensional models of a finite fault located in a half-space are constructed to study the ground motions from the 9 February 1971 earthquake as observed at JPL, Palmdale, and Lake Hughes (Array Station #4). The Cagniard-De Hoop Technique is used to compute the ground motions due to infinitesimal point sources which are evenly distributed (0.5 km spacing) on the fault plane. The responses are summed with time lags determined by the assumed hypocentral solution and rupture velocity. Nonuniform fault displacement is modeled by varying the weights of individual point sources. By investigating the motion due to small sections of the fault it is possible to understand how various wave types interfere to produce the motion due to the total fault. Recent modeling of teleseismic body waves by Langston has indicated that the fault changes dip from 50^{o} to 30^{o} at a depth of approximately 5 km. This feature has been incorporated into our models. The assumed fault geometry and station locations are shown in Figure 1. In Figure 2, we display assumed fault displacements for a preliminary model which is used to explain the motions at JPL, PLM, and LKH. The overall moment for this model is 1.5×10^{26} ergs. The hypocenter is assumed to lie in the region of maximum displacement and a rupture velocity of 1.8 km/sec (as suggested by Langston) is also assumed. Although stations LKH and JPL are situated at roughly equal epicentral distances, there appears to be a dramatic difference in the character and amplitudes of ground motion seen for these stations. This can be seen in Figures 3 and 4. In these figures, the synthetic ground motions for the fault model described above are compared with the integrated accelerograms for these stations. Because the integrated accelerograms have been filtered with an 8 sec. Ormsby filter, the synthetics are displayed both with and without the inclusion of this filter. Although it appears that the particular fault model used for Figures 3 and 4 is not, in detail, correct, it does well at explaining the differences in character and amplitude of ground motions as seen between JPL and LKH. An examination of Figure 5 helps one to appreciate the complex interplay between source and wave propagational effects. In this figure the fault is subdivided into 5 strips each of which has a width of 4 km. Also shown are synthetic motions (JPL, North) for a single point source located in the middle of each subfault. Although these point sources produce easily interpreted specific arrivals, it is clear that the JPL record results from complex and not easily interpreted interaction of both source and propagation effects. These synthetics also demonstrate the dramatic effect of the free-surface. Rayleigh wave and sP head wave contributions are of great importance.

The effects of even more complicated earth structure in these records is yet to be studied, but detailed synthesis of records for simpler aftershocks should add some insight to this problem.

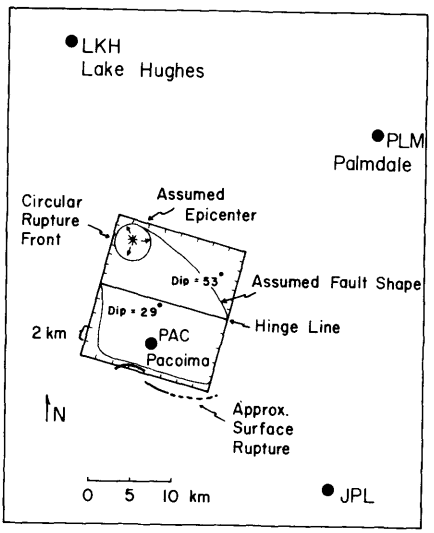

Fig. 1: Assumed geometry for the San Fernando fault and receivers. Model consists of a three dimensional finite fault in a half-space. A Green's function technique is used to integrate the exact solution for a point dislocation over the rectangular grid shown. A circular rupture front propagates from an assumed hypocenter and displacement magnitudes are prescribed on the fault surface.

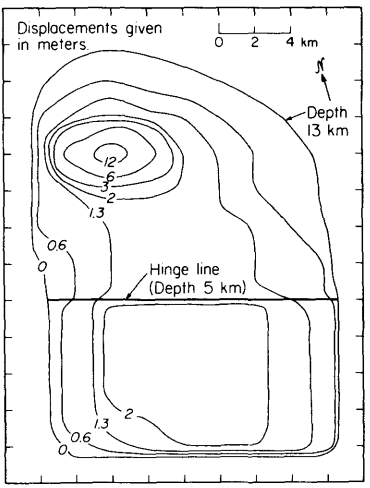

Fig. 2: Contour map of assumed fault displacements for the preliminary San Fernando model displayed in Figures 3, 4, and 5.

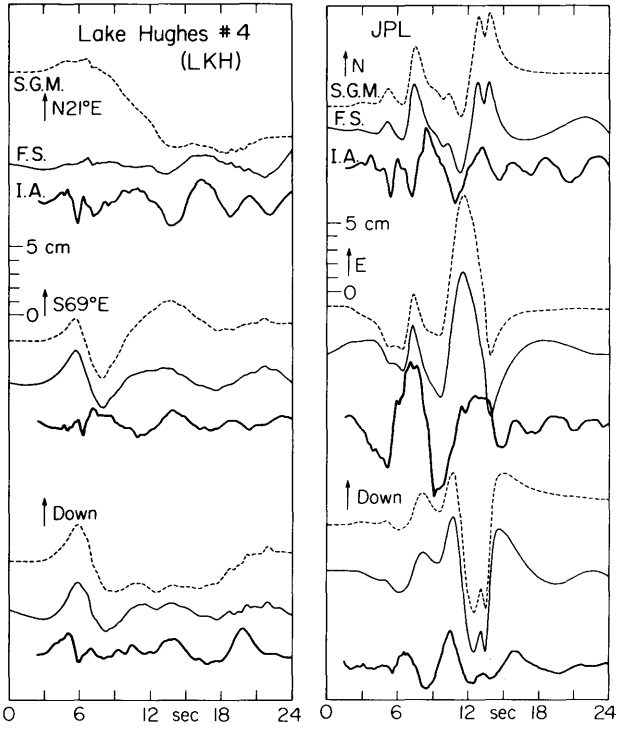

Fig. 3 and 4: Preliminary model of JPL and LKH displacement records. Massive faulting at depth of 13 km and a rupture velocity of 1.8 km/sec. are assumed. The top trace is the synthetic ground motion; the middle trace is the synthetic ground motion filtered with an 8 sec Ormsby filter; and the bottom trace is the observed displacement which has also been filtered at 8 sec. Notice the contrast between the records at JPL and LKH which lie at approximately equal epicentral ranges.

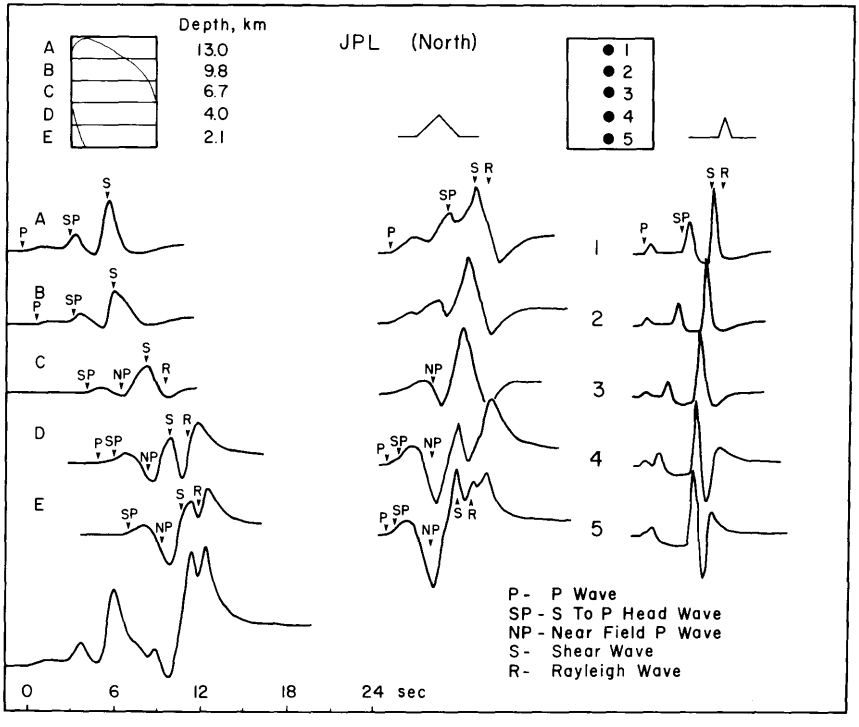

Fig. 5: Decomposition of the N component of synthetic ground motion for JPL. The finite fault is broken into 5 strips whose individual contributions are shown on the left. Responses of point sources which lie in the middle of these strips have been convolved with both 3 sec. and 0.8 sec. triangular far-field time functions and are displayed in the middle and on the right, respectively. By studying the point source responses, contributions of individual phases can be recognized in the synthetic for the finite fault. Notice the complex interplay of source and wave propagational effects.